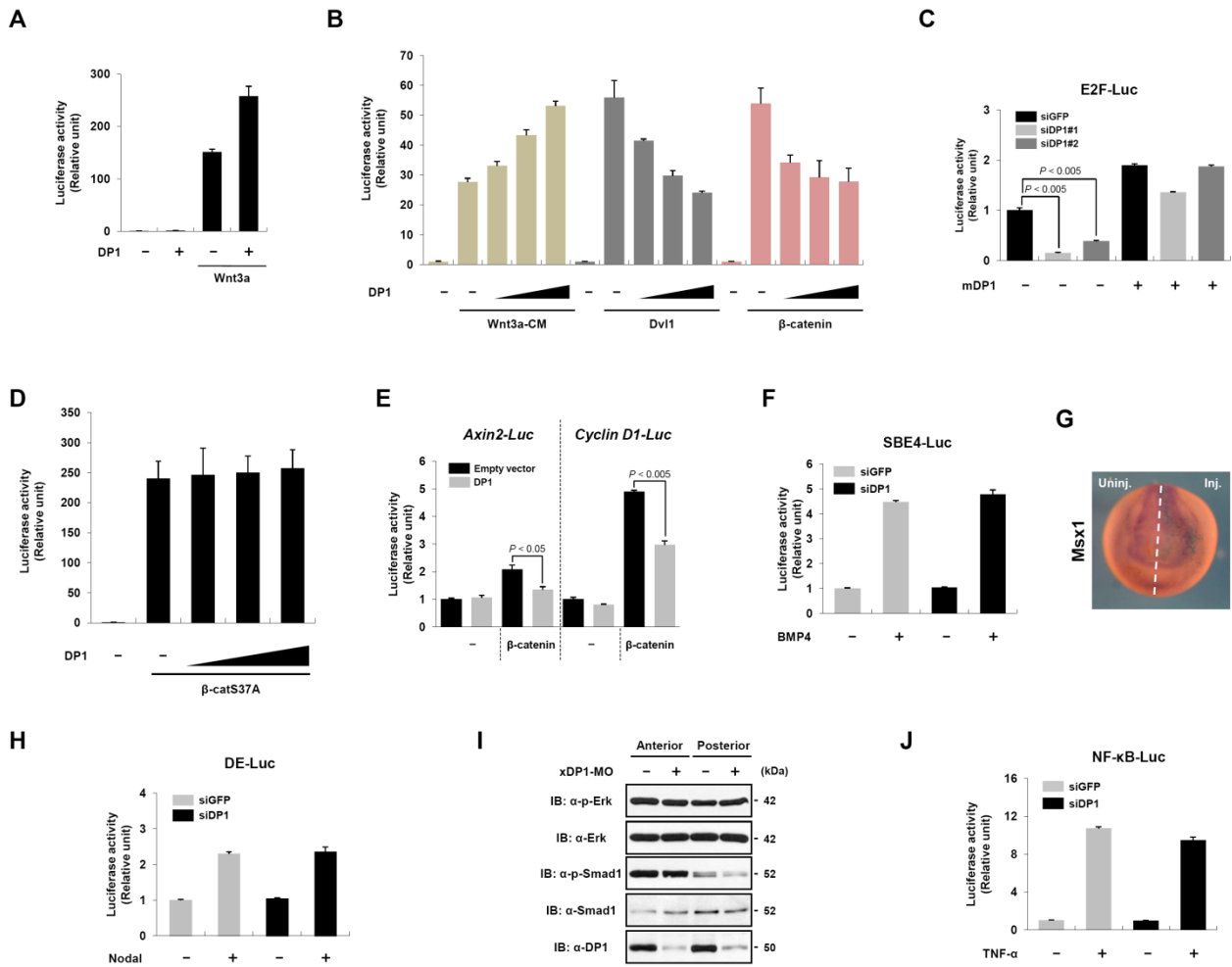


Supplementary Figure 1



**FIGURE S1. Specific regulation of Wnt signaling by DP1.**

(A) DP1 enhances TOP-FLASH activity induced by Wnt3a plasmid. (B) DP1 enhances TOP-FLASH activity induced by Wnt3a-CM but reduces Dvl- or  $\beta$ -catenin-mediated signaling activity. (C) Knockdown of DP1 decreases E2F1 signaling. E2F1 reporter activity was measured in HEK293T transfected with indicated siDP1s, and plasmids. Statistical significance (determined by Student's *t* test) is shown with the P value <0.005. (D) TOP-FLASH activity was measured in cells transfected with indicated plasmids. (E) Overexpression of DP1 attenuates  $\beta$ -catenin mediated Axin2 or Cyclin D1 promoter driven luciferase

activities. **(F)** BMP reporter (SBE-Luc) activities were measured in cells transfected with indicated plasmids including BMP4 expression plasmid. **(G)** A BMP target gene and a neural plate border marker, *Msx1* expression was analyzed by in situ hybridization from unilaterally xDP1-MO (40 ng) injected embryos. Note that the area of neural plate was expanded while the level of *Msx1* expression was not significantly perturbed on the injected side. **(H)** DP1 has no effect on Nodal signaling. Cells expressing siGFP or siDP1 with the DE-Luc plasmid were transfected with the Nodal construct and luciferase activity was measured. **(I)** Knockdown of DP1 in *Xenopus* embryo did not affect FGF-Erk signaling nor BMP-Smad1 signaling. xDP1-MO (60 ng) was bilaterally injected and dorsal explants were dissected, divided into anterior/posterior and subjected to western blot analysis with indicated antibodies. **(J)** NF- $\kappa$ B reporter (NF- $\kappa$ B-Luc) activities were measured in cells transfected with indicated plasmids and stimulated with recombinant TNF- $\alpha$  protein (10ng/ml). Data from all reporter assays represents average values from one representative experiment performed in triplicate. Error bars indicate standard deviations of triplicate.

## Supplementary Figure 2

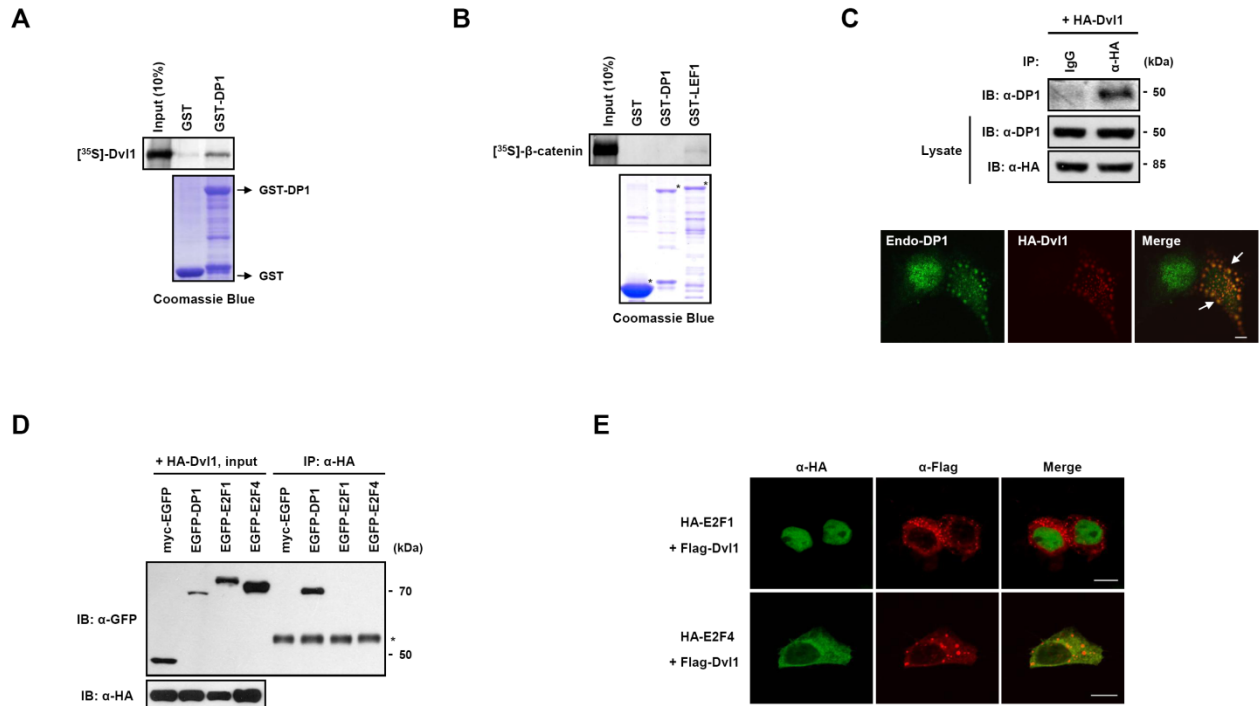


**FIGURE S2. DP1 interacts with Dvl1 independently of E2F.**

**(A)** *In vitro* binding assay of GST-DP1 and  $[^{35}\text{S}]\text{-Met}$  labeled Dvl1, visualized by autoradiography. **(B)** An *in vitro* binding assay between GST-DP1 or GST-LEF1, as a positive control, and  $[^{35}\text{S}]\text{-Met}$  labeled  $\beta\text{-catenin}$ . **(C)** IP and IF between HA-Dvl1 and endogenous DP1. Arrows indicate co-localized puncta. Scale bar, 10  $\mu\text{m}$ . **(D-E)** Dvl1 interacts and colocalizes only with DP1 but not with E2F proteins. Asterisk indicates IgG heavy chain. Scale bars indicate 10  $\mu\text{m}$ .

### Supplementary Figure 3

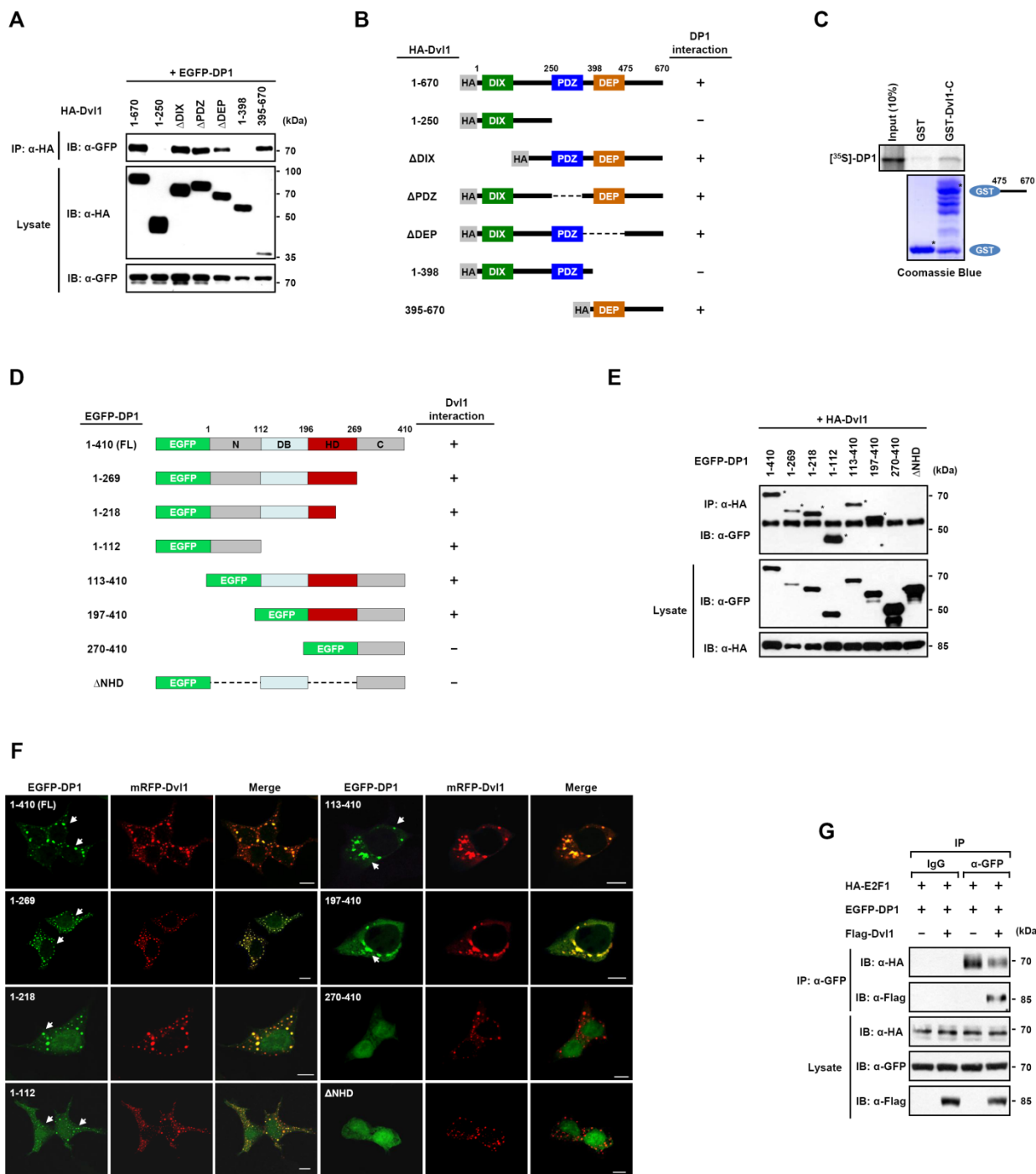


**FIGURE S3. Determination of domains for the interaction between Dvl1 and DP1.**

(A) HEK293T cells were cotransfected with different plasmid constructs as indicated. After 24h, cell lysates

were immunoprecipitated with anti-HA antibody, followed by Western blotting. **(B)** Summary of interaction between Dvl and DP1. The C-terminal region of Dvl is important for the interaction with DP1. **(C)** An *in vitro* binding assay between GST-Dvl-C (aa 475-670) and [<sup>35</sup>S]-Met labeled DP1. **(D)** Schematic diagrams of different DP1 deletion mutants used in the domain-mapping experiments. DP1 requires either its N-terminal region (aa 1-112) or heterodimerization region (aa 197-268) for the interaction with Dvl. **(E)** Both the N-terminus and heterodimerization regions of DP1 were sufficient to interact with Dvl1. **(F)** EGFP-DP1 truncation mutants, except aa 270-410 and ΔNHD, co-localize with Dvl. The scale bars indicate 10μm. **(G)** Dvl competes with E2F1 for the association with DP1. HEK293T cells expressing HA-E2F1 and EGFP-DP1 were transfected with or without Flag-Dvl. The interaction between DP1 and E2F1 was detected by immunoprecipitation with the anti-GFP but not control IgG antibody.

# Supplementary Figure 4

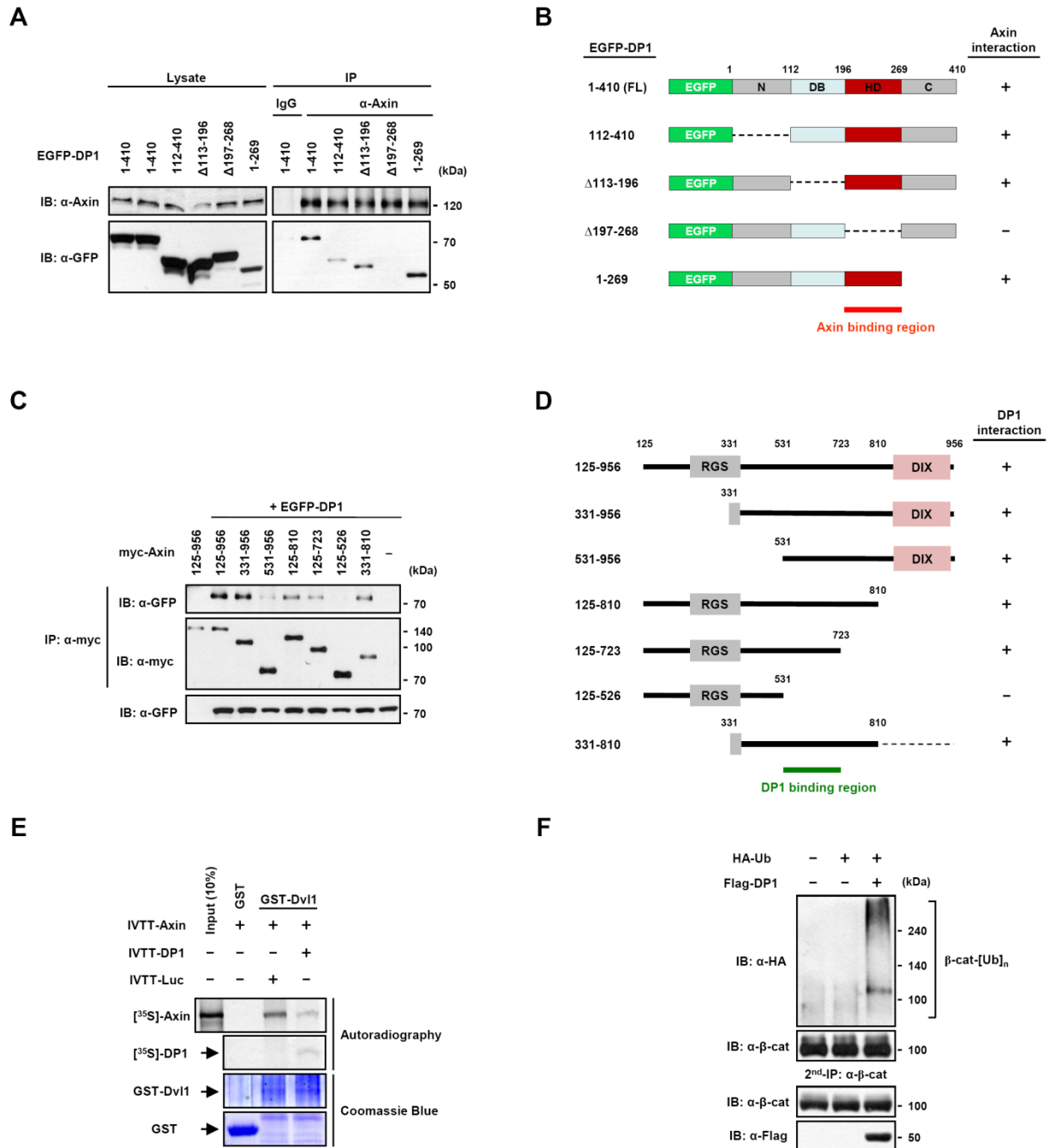


**FIGURE S4. Determination of domains for the interaction between Axin and DP1.**

(A) The heterodimerization region (aa 197-268) of DP1 is important for the interaction with Axin. DP1 constructs indicated in the figure were transiently transfected and whole cell lysates were subjected by

immunoprecipitation with anti-Axin antibody 24h after transfection, followed by Western blotting with anti-Axin and anti-GFP. **(B)** A schematic diagram of DP1 deletion constructs identifying the Axin-interacting region of DP1. **(C-D)** Mapping of the domain in Axin for the interaction with DP1. Axin interacts with DP1 via its aa 531-723-containing region. **(E)** Addition of *in vitro* translated DP1 reduces the interaction between Axin and GST-Dvl. Beads bound to GST or GST-Dvl1 were incubated with the *in vitro* translated Axin and the *in vitro* translated myc-DP1 or Luciferase. Interaction of GST-Dvl1 with Axin and the amount of myc-DP1 were visualized by autoradiography. The level of GST and GST-DV11 was detected by Coomassie Blue staining. **(F)** DP1 enhanced ubiquitination on  $\beta$ -catenin. HA-Ub was transfected with or without Flag-DP1. Cells were incubated in 10 mM MG132 for 4h, and the cell lysates were immunoprecipitated with anti- $\beta$ -catenin antibody. The immunoprecipitated products were boiled in 1% SDS to elute  $\beta$ -catenin from the beads and to break any protein-protein interactions. The supernatant was then collected and diluted 10 times in RIPA buffer, followed by immunoprecipitation with anti- $\beta$ -catenin antibody and immunoblotting with anti-HA antibody to detect  $\beta$ -catenin ubiquitination.

## Supplementary Figure 5

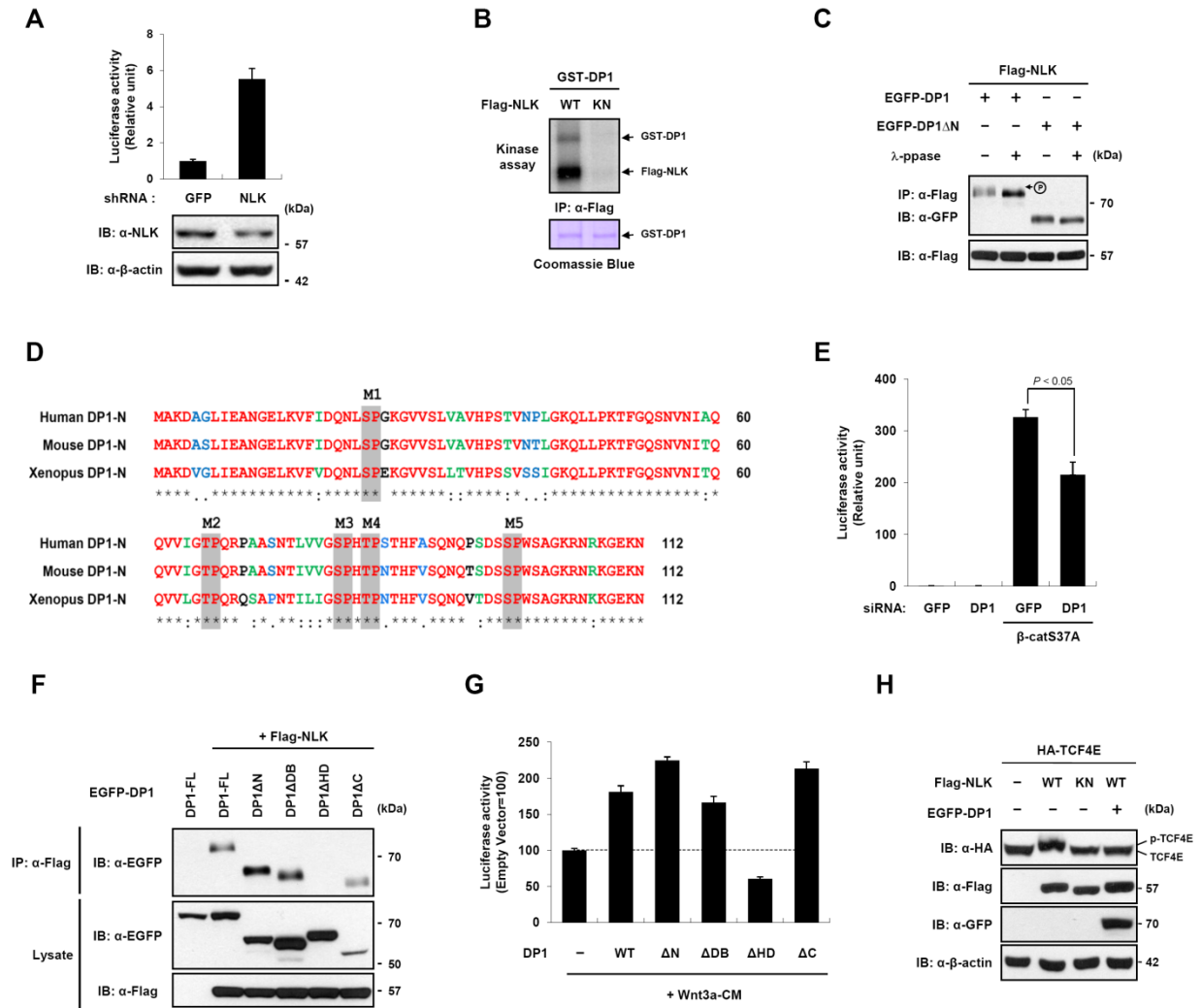


**FIGURE S5. DP1 positively regulates Wnt signaling in nucleus via inhibiting Tcf phosphorylation by NLK.**

(A) Knockdown of NLK in HEK293T cells resulted in TOP-FLASH activation. (B) DP1 is phosphorylated by NLK in vitro. The product of immunoprecipitation with anti-Flag antibodies from cell lysates of Flag-NLK or Flag-KN-NLK transfected HEK293T cells was incubated with GST-DP1. Phosphorylation was detected by autoradiography. (C) Elimination of the mobility shift by treatment with  $\lambda$  phosphatase. Flag-NLK was



transfected into HEK293T cells with EGFP-DP1 or EGFP-DP1 $\Delta$ N and the cell lysates were immunoprecipitated with anti-Flag antibodies. The immunoprecipitate was incubated with  $\lambda$  phosphatase and immunoblotting was performed with the indicated antibodies. **(D)** Alignment of the N-terminal region (aa 1-112) of DP1 from various organisms. Putative five conserved S/TP motifs are shaded in gray. **(E)** Knockdown of DP1 reduced  $\beta$ -catS37A mediated TOP-FLASH activity. **(F)** NLK interacts with DP1 via the HD region. Cells were transfected with EGFP-DP1 constructs and Flag-NLK. IP and immunoblotting were performed with the indicated antibodies. **(G)** Interaction of DP1 with NLK is required for the stimulation of Wnt3a-induced signaling. TOP-FLASH activities were measured in cells transfected with the indicated plasmids. Data are presented as means of three independent experiments. **(H)** DP1 restores the NLK-induced mobility shift of TCF4. HA-TCF4E was co-transfected with other plasmids as indicated. Cell lysates were immunoblotted with the indicated antibodies before the analysis of the Tcf4 mobility shift. Data from all reporter assays represents average values from one representative experiment performed in triplicate. Error bars indicate standard deviations of triplicate.

## Supplementary Figure 6

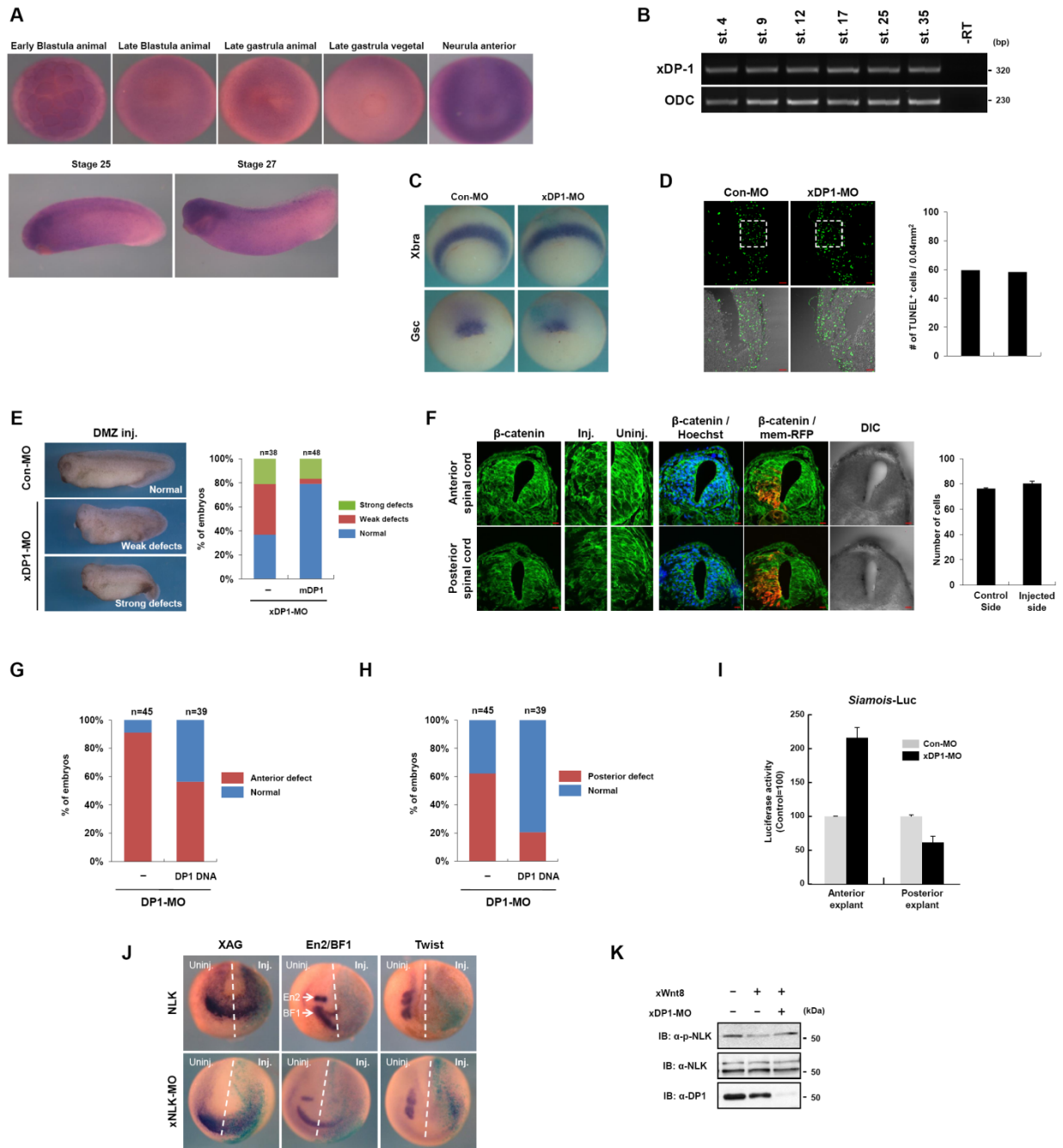


**FIGURE S6. *Xenopus* DP1 is expressed ubiquitously throughout development and loss of its function does not affect mesoderm induction and cell death.**

(A, B) Expression patterns of xDP1. xDP1 is expressed ubiquitously throughout development as revealed by

**(A)** *in situ* hybridization and **(B)** RT-PCR. ODC was used as a loading control. –RT: without reverse transcription. **(C)** Effects of xDP1-MO on mesodermal markers. Dorsal marginal two blastomeres of four-cell stage embryos were injected with control (Con-MO, 60 ng) or xDP1-MO (60 ng).  $\beta$ -galactosidase mRNA was co-injected as a lineage tracer. At the early gastrula stage (stage 11), embryos were subjected to *in situ* hybridization for *Xbra* and *Gsc*. **(D)** Effects of xDP1-MO on cell death. Dorsal animal two blastomeres of four-cell stage embryos were injected with control (Con-MO, 60 ng) or xDP1-MO (60 ng). At the neurula stage (stage 19), embryos were sagittally sectioned in paraffin and subjected to TUNEL assay with the *in situ* cell death detection kit (Roche). The images shown are focused on the anterior neural plate and endomesoderm. Positive signals were counted at 0.04 mm<sup>2</sup> window, focused on the anterior neural plate from six areas of two independent sections of both con-MO and xDP1-MO injected embryos. Average numbers of counting from six measurements were indicated. **(E)** Posterior defects of xDP1 morphants were rescued by MO-insensitive DP1 (Flag-mDP1). xDP1-MO (60 ng) was injected with and without Flag-mDP1 (2 ng) in dorsal marginal two blastomeres at 4-cell stage and cultured upto stage 37. Embryos with shortened axis and relatively normal tail were categorized as ‘Mild defects’ and those with shortened axis and almost no tail were categorized as ‘Severe defects’. **(F)** Subtle changes along the spinal cord were analyzed by cross section followed by immunostaining for  $\beta$ -catenin to mark cell boundary. xDP1-MO (45 ng) was injected with lineage tracer mem-RFP mRNA unilaterally and the injected embryos were fixed, embedded to paraffin, cross-sectioned and subjected to immunostaining at around stage 27. Note the irregular cell shape and neural tube boundary on the injected side both in the anterior and the posterior spinal cord sections. Cell numbers were

comparable for both control and injected side as counted from three independent sections. Error bars indicate standard deviations. **(G, H)** MO-insensitive DP1 plasmid DNA (Flag-mDP1 in pCS2 vector) significantly restored xDP1-MO induced anterior (G) and posterior (H) defects. **(I)** *Siamois* promoter driven luciferase activities were measured from anterior and posterior dorsal explants of control and DP1 morphants. Samples were divided into three pools of ten explants each for statistical analysis (See Materials and Methods, *Xenopus* embryos manipulation). **(J)** Effects of NLK overexpression and knockdown on anteroposterior neural markers. mNLK (4 ng) or xNLK-MO (5 ng) was injected unilaterally and the expression of XAG, En2, BF1 or Twist was assessed by in situ hybridization. **(K)** NLK phosphorylation was suppressed by xWnt8 and the suppression was rescued by xDP1-MO in the *Xenopus* posterior dorsal explants. xWnt8 (10 pg) and xDP1-MO (60 ng) were injected bilaterally as indicated. Posterior dorsal explants were dissected at stage 13 and subjected to western blot with indicated antibodies.

## Supplementary Figure 7

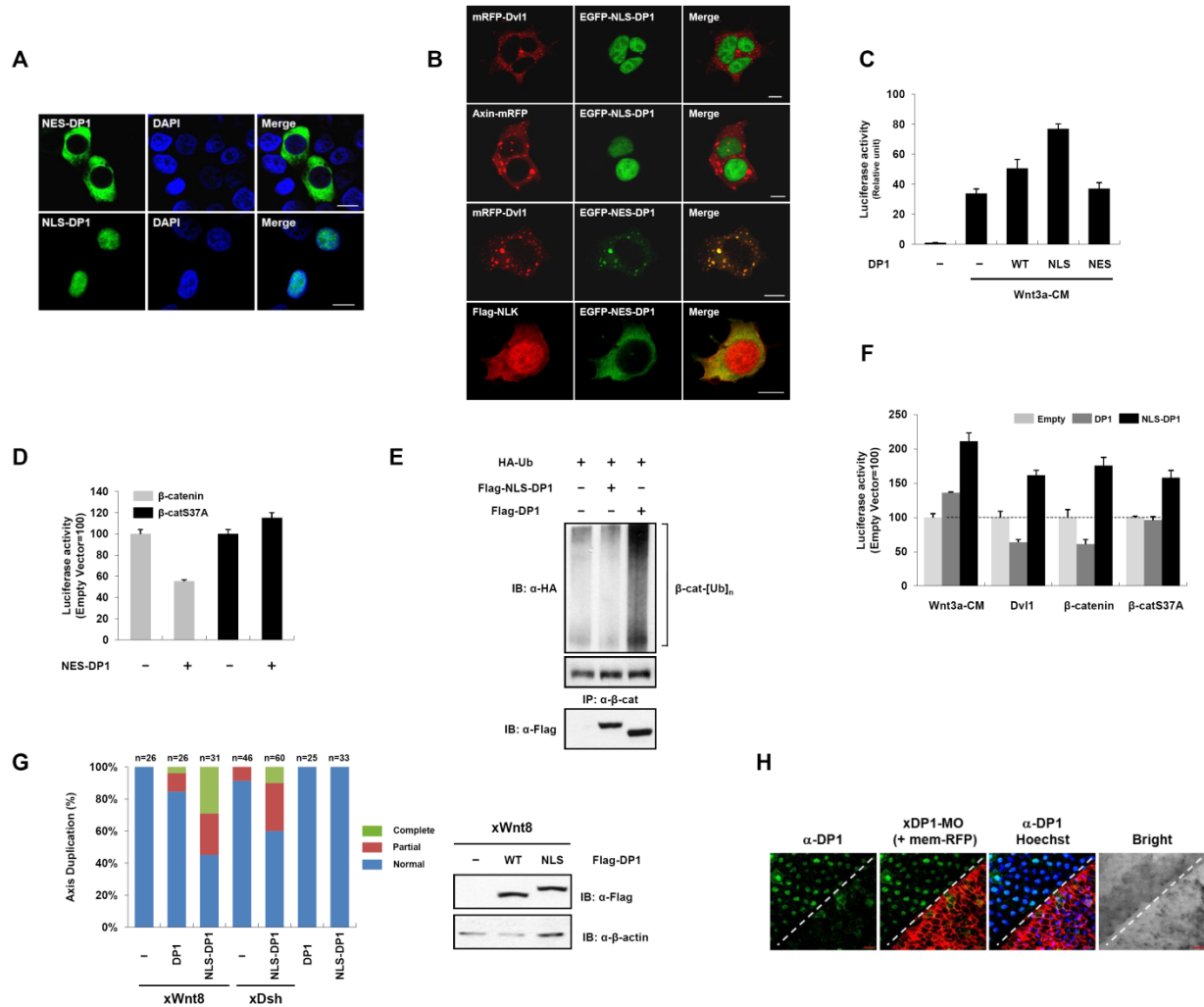


**FIGURE S7. The dual roles of DP1 in Wnt/ $\beta$ -catenin signaling are determined by differential nucleocytoplasmic localizations of DP1.** (A) NLS-DP1 mainly localizes in nucleus, and NES-DP1 in the cytoplasm. Scale bars indicate 10 $\mu$ m. (B) NLS-DP1 did not interact with Dvl1 or Axin. NES-DP1 colocalized with Dvl1 in similar to wild-type DP1, whereas it has no influence on the expression pattern of NLK. (C) NLS-DP1, but not NES-DP1, has a stronger ability to enhance Wnt3a-induced TOPFLASH activity than wild-type DP1. HEK293 cells, co-transfected with DP1 constructs and the Wnt reporter plasmid, were incubated with the Wnt3a conditioned medium before measuring the luciferase activity. (D) NES-DP1 is still able to

suppress TOP-FLASH activation induced by  $\beta$ -catenin but not by  $\beta$ -catS37A. **(E)** TOP-FLASH activities were measured in cells transfected with indicated plasmids and/or treated with Wnt3a-CM. The error bars indicate standard deviations of triplicate. **(F)** NLS-DP1 does not induce the poly-ubiquitination of  $\beta$ -catenin. **(G)** Axis duplication assay in *Xenopus*. Sub-optimal doses of xWnt8 (1 pg) and xDsh (250 pg) were injected with DP1 (1 ng) and NLS-DP1 (1 ng), as indicated. Right panel shows that the injected RNAs produced roughly equal amounts of proteins. **(H)** Specificity test of the anti-mouse DP1 antibody ( $\alpha$ -DP1, Santa Cruz). xDP1-MO (45 ng) was co-injected with a lineage tracer mem-RFP mRNA into one blastomere of two-cell stage embryo. At the neurula stage (stage 15), dorsal explants was dissected and subjected to immunostaining with  $\alpha$ -DP1, followed by Hoechst staining. *Xenopus* DP1 protein was efficiently recognized only on the control side (xDP1-MO uninjected side). Dashed lines correspond to the midline. Scale bar, 20  $\mu$ m. Data from all reporter assays represents average values from one representative experiment performed in triplicate. Error bars indicate standard deviations of triplicate.

## Supplementary Figure 8

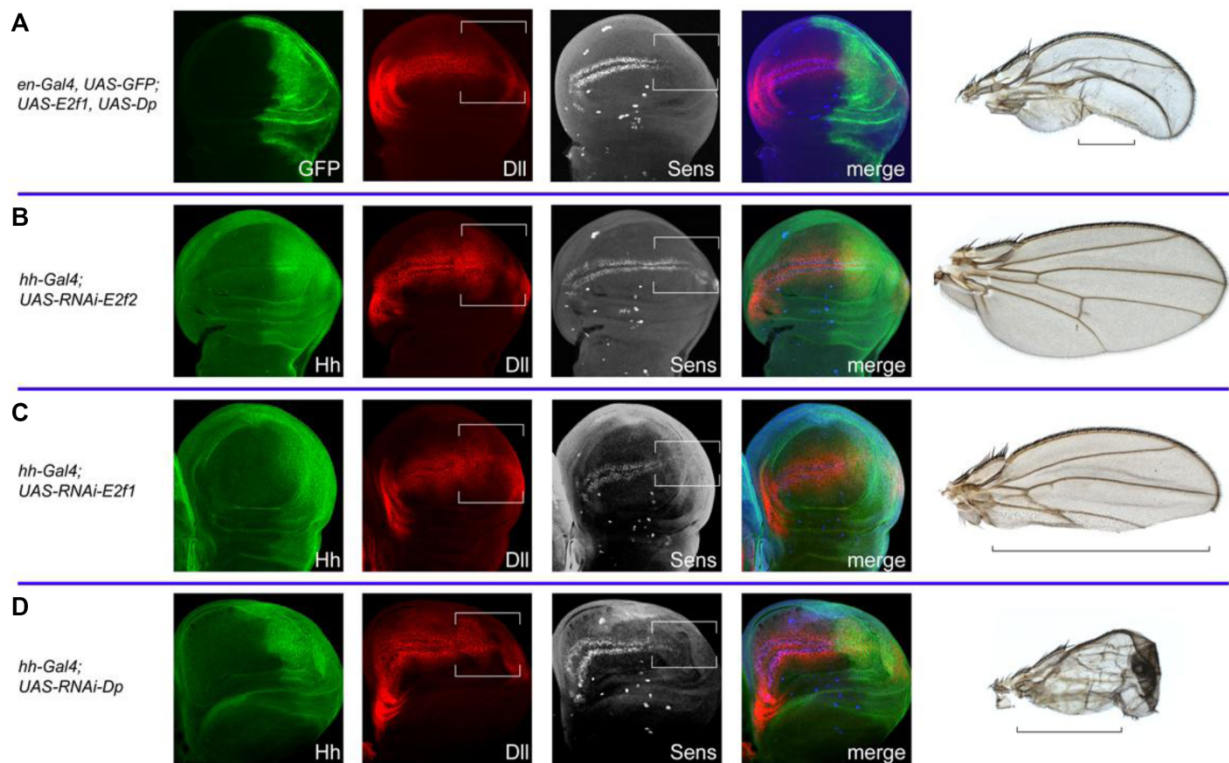


**FIGURE S8. Both overexpression and downregulation of Dp and E2f1 decrease Wingless signaling in *Drosophila* wings.**

(A) Overexpression of Dp and E2f1 in the posterior compartment (marked by GFP staining) results in a decrease in expression of the Wingless low-threshold target gene Distal-less (Dll, red) and loss of the high-threshold target gene Senseless (Sens, grey) in third instar larval wing imaginal discs. In the adult wings this results in loss of posterior wing margin structures (marked by a bar). (B-C) RNAi-mediated downregulation of Dp (D) and E2f1(C), but not E2f2 (B) in the posterior domain (marked by anti-Hedgehog staining, Hh, green) leads to similar phenotypes. Note that the *RNAi-Dp*-expressing flies die as pharate adults and have to be extracted from the pupal cases for wing inspection, resulting in the general abnormal appearance of these wings.

## Materials and Methods

### *Drosophila* experiments

*UAS-RNAi* lines targeting *Dp*, *E2f1*, and *E2f2* (Dietzl et al, 2007) were expressed under the control of the *hh-Gal4* line (Tanimoto et al, 2000) driving expression in the posterior compartment. Similar expression of *UAS-E2f1*, *UAS-Dp* (Neufeld et al, 1998) was lethal; thus a weaker driver line, *en-Gal4; UAS-GFP* (Greco et al, 2001) expressing in the same pattern, was selected for the overexpression experiments. Flies were maintained at 25°C. Wing imaginal discs and adult wings were processed as in (Katanaev et al, 2005). The following primary antibodies were used in the immunostaining: guinea pig anti-Sens 1:1000 (Nolo et al, 2000), mouse anti-Dll at 1:1000 (gift of G. Struhl), rabbit anti-Hh (NHhI) 1:1000 (Takei et al, 2004). Cy3- and Cy5-labeled (Jackson ImmunoResearch) and Alexa Fluors 405 (Invitrogen) secondary antibodies were used.

### Supplementary references

Dietzl G, Chen D, Schnorrer F, Su KC, Barinova Y, Fellner M, Gasser B, Kinsey K, Oppel S, Scheiblauer S, Couto A, Marra V, Keleman K, Dickson BJ (2007) A genome-wide transgenic RNAi library for conditional gene inactivation in *Drosophila*. *Nature* **448**: 151-156

Greco V, Hannus M, Eaton S (2001) Argosomes: a potential vehicle for the spread of morphogens through epithelia. *Cell* **106**: 633-645



Katanaev VL, Ponzielli R, Semeriva M, Tomlinson A (2005) Trimeric G protein-dependent frizzled signaling in *Drosophila*. *Cell* **120**: 111-122

Neufeld TP, de la Cruz AF, Johnston LA, Edgar BA (1998) Coordination of growth and cell division in the *Drosophila* wing. *Cell* **93**: 1183-1193

Nolo R, Abbott LA, Bellen HJ (2000) Senseless, a Zn finger transcription factor, is necessary and sufficient for sensory organ development in *Drosophila*. *Cell* **102**: 349-362

Takei Y, Ozawa Y, Sato M, Watanabe A, Tabata T (2004) Three *Drosophila* EXT genes shape morphogen gradients through synthesis of heparan sulfate proteoglycans. *Development* **131**: 73-82

Tanimoto H, Itoh S, ten Dijke P, Tabata T (2000) Hedgehog creates a gradient of DPP activity in *Drosophila* wing imaginal discs. *Mol Cell* **5**: 59-71